

Ring-Like Solitons in Plasmonic Fiber Waveguide Composed of Metal-Dielectric Multilayers

Jie-Yun Yan^{1,*}, Lu Li,² and Jinghua Xiao¹

¹*School of Science, Beijing University of Posts and Telecommunications, Beijing 100876, People's Republic of China and*

²*Institute of Theoretical Physics, Shanxi University, Taiyuan 030006, People's Republic of China*

We design a plasmonic fiber waveguide (PFW) composed of coaxial cylindrical metal-dielectric multilayers in nanoscale, and constitute the corresponding dynamical equations describing the modes of propagation in the PFW with the Kerr nonlinearity in the dielectric layers. The physics is connected to the discrete matrix nonlinear Schrödinger equations, from which the highly confined ring-like solitons in scale of subwavelength are found both for the visible light and the near-infrared light in the self-defocusing condition. Moreover, the confinement could be further improved when increasing the intensity of the input light due to the cylindrical symmetry of the PFW, which means both the width and the radius of the ring are reduced.

PACS numbers: 73.20.Mf, 78.67.Pt, 42.65.Tg

How to control the propagation of the light is a most important subject in optics. Using the technology of the optical fiber waveguides (OFWs) to pilot the light is a big advance towards all-optical signal processing. When consider ever-accelerated miniaturization of optical devices, however, the conventional OFWs seem to be difficult to fulfill the requirement because of the diffraction limitation for the optical components of dielectric photonic materials. Recently, it is shown that the limitation may be overcome in the rapid developing field of plasmonics[1–3] based on properties of the surface plasmon polariton (SPP), a confined mode localized at the interface of metal and dielectric material [4, 5]. Subsequently wide attentions have been paid to miscellaneous nanostructures with metamaterials involved in pursuit of subwavelength confinement of the light[6]. Among these progresses, several researchers have predicted the subwavelength control of the light in various lattices through the formation of solitons when the nonlinearity is considered. It has been found that the planar nonlinear metal-dielectric multilayers (MDM), a stack of alternating metal-dielectric nanolayers, can effectively manipulate the propagation of light[7–9] and put a subwavelength confinement on it [10–15]. For instance, Zhang's group theoretically found the subwavelength discrete soliton in the nanoscaled periodic structures consisting of MDM[14]. Ye *et al.* predicted the stable fundamental and vortical plasmonic lattice solitons of subwavelength extent in arrays of metallic nanowires embedded in a nonlinear medium[15].

Then could we construct a kind of waveguide in analogy to the optical fiber waveguide to control the light's propagation in two-dimensional (2D) transverse space based on the plasmonics rather than the optics? In this Letter we design a plasmonic fiber waveguide (PFW) by rolling the MDM to a cylindrical shape to guide the light. The nonlinearity in the dielectric layers are employed to realize the subwavelength confinement in radial direction when propagating along the axial direction. Based on

the advanced nano-technologies[16–18] in addition to the sophisticated fiber fabrications, this kind of PFW is supposed to be a easily-fabricated structures. Actually a spherical hyperlens made of the MDM has been realized in experiment[19]. Besides, in contrast to the lattices made of planar MDM, the PFW has the cylindrical symmetry, which produces the centripetal confinement in the form of solitons. Our results show that the energy could be highly confined in the cross section with size far small than the operating wavelength. This kind of confinement combines the advantages of fiber's long distance transportation and minimized transverse space caused by the cooperation of nonlinearity and SPP's field enhancement effect, which is significant for applications of plasmonics in future communication and large-scale integration.

Our structure of the PFW is composed of alternating metal and dielectric coaxial cylindrical layers, as shown in Fig. 1(a) and (b), where the coaxial cylindrical metal layers are labeled as $n = 1, 2, \dots$ along radial direction. The thicknesses of the metal layer and the dielectric layer are represented by w and d , respectively. Note that the dielectric material at center is a cylinder with the radius of d . The dielectric constants of metal and dielectric material are $\epsilon_0\epsilon_m$ and $\epsilon_0\epsilon_d$, respectively, with ϵ_0 is dielectric constant of the vacuum. A set of typical parameters used in the Letter are that: the metallic dielectric constant is Johnson's data for the metal Ag [20], the dielectric constant for the dielectric material is 10, and their thicknesses are $w = 10\text{nm}$ and $d = 40\text{nm}$, respectively. In fact, the following theory is still applicable when the parameters d and w are functions of n .

When the light wave with the frequency ω propagates in the PFW, the SPP modes are excited at each interface[21]. Therefore the PFW can be considered as an plasmonic multiwaveguide system, of which the i -th single plasmonic waveguide (SPW) is constituted by the corresponding i -th coaxial metal sheathes and the dielectric environment. The interaction among the propagating modes of SPPs in these SPWs would cause the energy

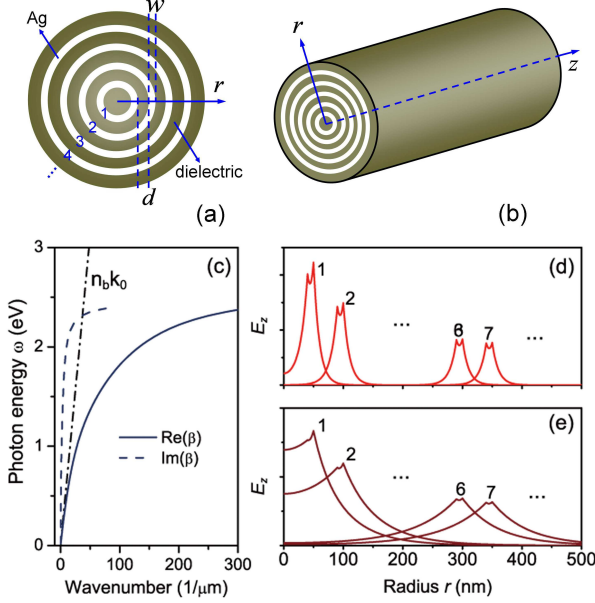


FIG. 1: (a) Cross section of the PFW; (b) Schematics of the PFW; Only first few metallic layers are draw for demonstration. (c) Dispersion of SPP mode in the 1-th SPW. E_z distributions in different SPWs in case of $\lambda = 700$ nm (d), and $\lambda = 1550$ nm (e), respectively. For clarity, only that in SPWs with indexes 1, 2, 6, and 7 are draw.

diffraction if no other mechanism counteracts it, as shown below. We then start by exploring the guiding modes in each SPW to gain some insights. By exactly solving the Maxwell equations, we can get the dispersion relation and field distributions $[\mathbf{E}^{(n)}(r), \mathbf{H}^{(n)}(r)]$ of the SPP mode in n -th SPW. Here we only consider the fundamental TM mode of SPP with nonvanishing components $E_z^{(n)}$, $H_\phi^{(n)}$ and $E_r^{(n)}$, which are functions of the radial coordinate r . The dispersion relation of 1-th SPW is given in Fig. 1(c), where β is the propagation constant of the SPP, n_b is the refractive index of the environment, and k_0 is the wavenumber in vacuum. The dot-dash line labeled by $n_b k_0$ is the dispersion of the light in the background. From Fig. 1(c) one can see that the propagation constant β has a strong dependence on the frequency and the real part is always bigger than that of the background, which is the characteristics of the SPP. Calculations show that β_n have a small variation for a given frequency, especially for the SPWs with high index, which is reasonable as the high-index SPWs can be approximated as planar waveguides with the same width of w . The field distributions of the SPP modes in different SPWs is sensitive to the frequency. For example, $E_z^{(n)}$ ($n = 1, 2, \dots, 6, 7, \dots$) are plotted in Fig. 1(d) for $\lambda = 700$ nm and in Fig. 1(e) for $\lambda = 1550$ nm. It is clear that the interaction between adjacent modes in case of $\lambda = 700$ nm is small enough to take a nearest-neighbor approximation while it is not in

case of $\lambda = 1550$ nm.

For the whole PFW, we can express the total electric field $\mathbf{E}(r, z)$ and magnetic field $\mathbf{H}(r, z)$ in the superposition of the modes in all SPWs: $E_r = \sum_n a_n(z) E_r^{(n)} e^{-i\omega t}$, $E_z = \sum_n a_n(z) \frac{\epsilon^{(n)}}{\epsilon} E_z^{(n)} e^{-i\omega t}$, and $H_\phi = \sum_n a_n(z) H_\phi^{(n)} e^{-i\omega t}$, where a_n is the mode amplitude of the n -th SPW, ϵ and $\epsilon^{(n)}$ are the dielectric constant of the PFW and of n -th SPW, respectively. For simplicity all these modes of SPWs have been normalized by their energy flow $I_n = \frac{1}{2} \int_S \text{Re}(\mathbf{E}^{(n)*} \times \mathbf{H}^{(n)}) \cdot \mathbf{e}_z dS$ here. Thus the equation describing the dynamics of the mode amplitudes a_n can be determined by the generalized Lorentz reciprocity theorem[22], which can be written as:

$$i \frac{d}{dz} \mathbf{C} \mathbf{A} + (\mathbf{B} \mathbf{C} - \mathbf{K}) \mathbf{A} - \mathbf{\Gamma} |\mathbf{A}|^2 \mathbf{A} = 0, \quad (1)$$

where \mathbf{A} is a vector given by the elements a_n ($n = 1, 2, \dots$) and $|\mathbf{A}|^2$ represents a diagonal matrix with corresponding elements $|a_n|^2$. Matrix \mathbf{B} is a diagonal matrix with the elements given by the propagation constants β_n . \mathbf{C} , \mathbf{K} and $\mathbf{\Gamma}$ are matrices, whose elements are defined respectively by

$$C_{n,n'} \equiv \frac{1}{4} \int_S (E_r^{(n')} H_\phi^{(n)} + E_r^{(n)} H_\phi^{(n')}) dS, \quad (2)$$

$$K_{n,n'} \equiv \frac{\omega}{4} \int_S (\epsilon^{(n)} - \epsilon) \tilde{K}_{n,n'} dS, \quad (3)$$

$$\Gamma_{n,n'} \equiv \int_S \frac{-\epsilon_0 \xi \epsilon_d^2 \alpha_{n'} \omega}{4} \tilde{K}_{n,n'} dS, \quad (4)$$

where $\tilde{K}_{n,n'} = E_r^{(n')} E_r^{(n)} - \frac{\epsilon^{(n')}}{\epsilon} E_z^{(n')} E_z^{(n)}$, $\alpha_n = |E_r^{(n)}|^2 + |\frac{\epsilon^{(n)}}{\epsilon} E_z^{(n)}|^2$.

In the above derivation for Eq. (1), the change of relative dielectric constant ϵ_d due to the introduced nonlinearity in the dielectric layers is $\xi \epsilon_d^2 |E|^2$ with the Kerr coefficient ξ . Also, we have neglected the nonlinear interaction among the SPWs, i.e. items including $|a_{n'}|^2 a_n$ ($n \neq n'$) are neglected. If the distance d is big enough so that the overlapping of adjacent SPWs' fields can be ignored, the matrix \mathbf{C} can also be approximated as a diagonal matrix, as shown in Ref. [15]. But for the case of strong interaction, as the case shown in Fig. 1(e), the approximation is not acceptable. Therefore the Eq. (1) is suitable to more general cases, which can also be written as a more simplified form

$$i \frac{d}{dz} \mathbf{A} + \mathbf{T} \mathbf{A} + \mathbf{G} |\mathbf{A}|^2 \mathbf{A} = 0, \quad (5)$$

where $\mathbf{T} \equiv \mathbf{C}^{-1} \mathbf{B} \mathbf{C} - \mathbf{C}^{-1} \mathbf{K}$ and $\mathbf{G} \equiv -\mathbf{C}^{-1} \mathbf{\Gamma}$. This is discrete matrix Schrödinger equations. For the parameters we adopted, we find that matrix \mathbf{T} and \mathbf{G} can be approximated as a triple diagonal matrix and a diagonal

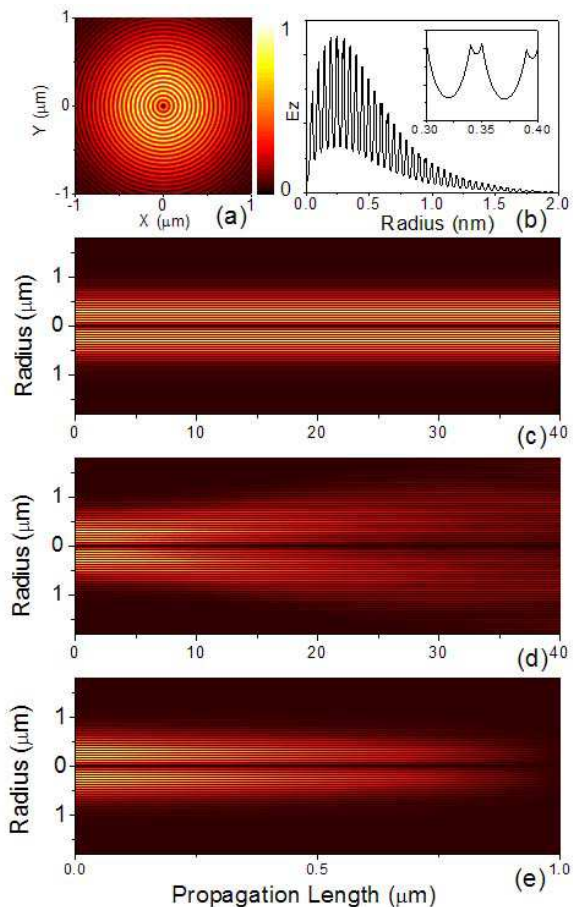


FIG. 2: (color online)(a) the profile of the amplitude of the longitudinal field component E_z of the soliton with the wavelength of $\lambda = 700$ nm in the PFW. (b) the distribution of E_z along the radial direction, inset is an amplification of one part for clarity. (c) The nonlinear (soliton) and (d) the linear propagation over $40 \mu\text{m}$ distance in lossless PFW. (e) The propagation of the soliton in the same PFW when the loss in metal is taken into account.

one, respectively. Neglected elements are at least one order of magnitude less than others. Then it is reduced to the nonsymmetric discrete nonlinear Schrödinger equations with variable nonlinear coefficients. In the equations, the matrix \mathbf{T} is determined by the interaction between the SPP mode in each SPW with its counterpart in the inner nearest SPW and outer one. Due to the cylindrical symmetry of the PFW, \mathbf{T} is nonsymmetric matrix, which leads to the different diffraction towards the center or outside. The matrix $\mathbf{\Gamma}$ governs the nonlinearity, which will balance the diffraction when solitons forms. The elements $|G_n|$ ($n = 1, 2, \dots$), proved to decrease with the n index, give a centripetally increasing nonlinearity. Both these characteristics contribute to the highly confined solitons in the PFW.

We sought the soliton solutions in the form of $a_n(z) = \sqrt{I_0} u_n e^{i\rho z}$, where the amplitudes u_n and ρ are both in-

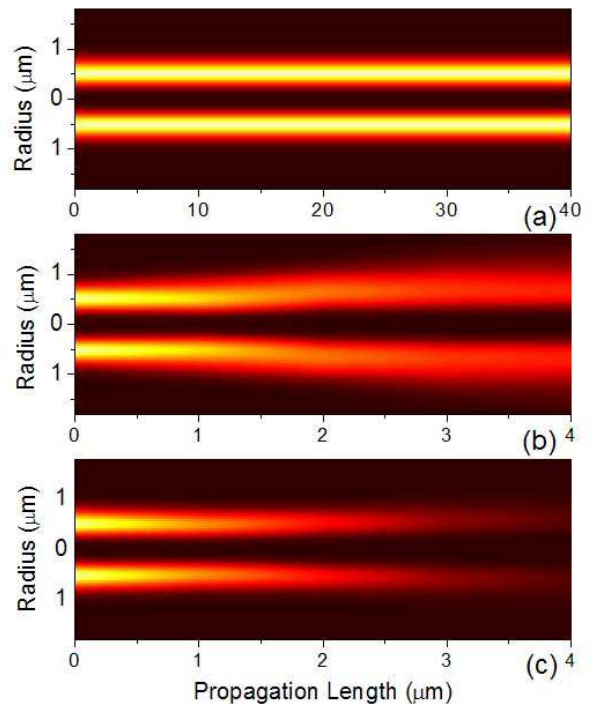


FIG. 3: (a) The propagation of soliton along $40 \mu\text{m}$ in the lossless PFW when the wavelength λ is 1550nm . (b) Linear propagation along $4 \mu\text{m}$ in the same PFW. (c) The propagation of the soliton along $4 \mu\text{m}$ when the loss is considered.

dependent of z . We also define the intensity as $I = \sum_n |a_n|^2$ in the solution. We put our emphasis on the unstaggered solitons[14] formed in the self-defocusing media, with the Kerr coefficient set as $-1 \times 10^{-15} \text{m}^2/\text{V}^2$ and I_0 about $5 \times 10^{-4} \text{W}$. The number of layers is chosen big enough to ensure the fields vanishing at the boundary.

Fig. 2(a) plots the profile of the amplitude of the longitudinal field component E_z of the soliton in the PFW with $I = 0.05I_0$ and Fig. 2(b), with an amplification of one part, presents the distribution of E_z along the radial direction in the case of $\lambda = 700$ nm. As E_z reflects the intensity of the light, we can conclude from Fig. 2(a) that the energy mainly concentrates inside the region with the radius of about 400 nm. It is noteworthy that the maximal intensity is at the circle with radius about 250 nm other than at the center, which could be seen it more clearly from Fig. 2(b). That is why we call it as the ring-like solitons. It is the nonlinearity that confines the energy in a region with the size of subwavelength, where the effect of field enhancement provided by the SPPs is prominent, which in turn makes the nonlinearity more achievable. The cylindrical symmetry enable energy to concentrate towards the axis, which further facilitates the confinement of energy. The linear case where the diffraction dominates are also plotted in Fig. 2(d) for comparison. Moreover, Fig. 2(b) also shows that metal

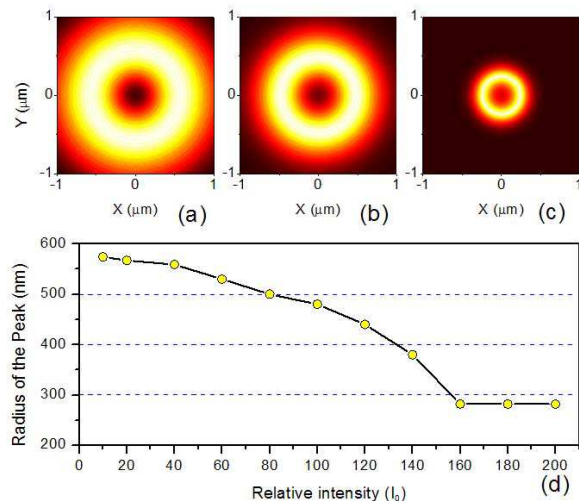


FIG. 4: (a-c) The profiles of the solitons with the intensity of $20I_0$, $100I_0$, $180I_0$ respectively. The values in each figure have been normalized to their maximum. (d) Radius of the soliton's peak changing with the intensity.

layers hold a large portion of the energy. For this reason in addition to a relative big value of $\text{Im}[\beta_n]$ for visible light, the soliton experiences a high loss in the PFW if the loss in the metal is considered, as shown in Fig. 2(e). A gain medium is consequently necessary for the PFW working on the visible lights.

In the case of $\lambda = 1550$ nm, the ring-like solitons are also found in the same PFW. Its propagation along $40\mu\text{m}$ in the lossless situation with $I = 80I_0$ is plotted in Fig. 2(a), while the lossless linear propagation is shown in Fig. 2(b). Compared with the case of $\lambda = 700$ nm, the diffraction is outstanding, because of the remarkable overlapping between the adjacent SPWs' fields and thus a strong interaction among the SPPs in different SPWs, as we discussed before. And consequently the highly confined soliton is achieved with a relative strong intensity. However, as the portion of the field residing inside the metal layers decreasing correspondingly, the transmission distance is enlarged to some extent in the lossy PFW, which is clearly seen by comparing Fig. 3(c) with Fig. 2(e).

For the lattices solitons, increasing both the intensity and the nonlinear coefficient will enhance its nonlinear effect and therefore make the energy more confined. In the PFW, this characteristics is particularly obvious. The profiles of the solitons under three values of the intensity $I = 20I_0$, $100I_0$, $180I_0$ are drawn in Fig. 4(a)-(c). The energy of the soliton is confined in a ring of less and less width with the increasing of intensity. Furthermore, because of the nonsymmetry of the matrix \mathbf{T} , increasing the intensity also makes the energy moving centripetally. It is an exciting result that the highly confined 2D soliton in Fig. 4(c) has a transverse size far smaller than the

wavelength. The peaks of these solitons with more values of intensities are plotted in Fig. 4(d). Calculation shows that when the intensity reaches a certain value, the peak stops moving. The reason is that in this situation the nonsymmetry of the diffraction is trivial for the considerable nonlinearity. Besides, as the matrixes \mathbf{T} and \mathbf{G} are determined by the field distribution of SPWs, the soliton shape could be modified by adjusting the radius and width of each metal layer.

In conclusion, we designed a PFW composed of the MDM and predicted theoretically the form of highly confined subwavelength solitons in the PFW with Kerr nonlinearity both for the visible light and the near-infrared light. The equations describing the solitons have been obtained in an compact matrix form. This kind of PFW is expected to take the role of OFW in future in the plasmonics-based communications and other nanophotonic applications, such as lithography, beam shaping, *et al.*

This work is supported by the National Natural Science Foundation of China (Grant Nos. 11004015 and 61078079), National Basic Research Program of China (Grand No. 2010CB923200), and the Doctoral Fund of Ministry of Education of China (Grant No. 20100005120017).

*Email: jyyan@bupt.edu.cn

-
- [1] S. A. Maier, M. L. Brongersma, P. G. Kik, S. Meltzer, A. A. G. Requicha, and A. Atwater, *Adv. Mater.* **13**, 1501 (2001).
 - [2] S. A. Maier, *Current Nanoscience* **1**, 17 (2005).
 - [3] D. K. Gramotnev, and S. I. Bozhevolnyi, *Nature Photonics* **4**, 83, (2010).
 - [4] J. M. Pitarke, V. M. Silkin, E. V. Chulkov, and P. M. Echenique, *Rep. Prog. Phys.* **70**, 1 (2007).
 - [5] W. L. Barnes, A. Dereux, and T. W. Ebbesen, *Nature (London)* **424**, 824 (2003).
 - [6] B. Lee, I. M. Lee, S. Kim, D. H. Oh, and L. Hesselink, *J. Mod. Opt.* **57**, 1479 (2010).
 - [7] A. Husakou, and J. Herrmann, *Phys. Rev. Lett.* **99**, 127402 (2007).
 - [8] S. M. Vuković, Z. Jakšić, I. V. Shadrivov, Y. S. Kivshar, *Appl. Phys. A* **103**, 615 (2011).
 - [9] C. W. Lin, K. P. Chen, C. N. Hsiao, S. Lin, C. K. Lee, *Sensors and Actuators B* **113**, 169 (2006).
 - [10] O. Peleg, M. Segev, G. Bartal, D. N. Christodoulides, and N. Moiseyev, *Phys. Rev. Lett.* **102**, 163902 (2009).
 - [11] I. Avrutsky, I. Salakhutdinov, J. Elser, and V. Podolskiy, *Phys. Rev. B* **75**, 241402(R) (2007).
 - [12] G. Bartal, G. Lerosey, and X. Zhang, *Phys. Rev. B* **79**, 201103 (2009).
 - [13] Y. V. Kartashov, B. A. Malomed, and L. Torner, *Rev. Mod. Phys.* **83**, 247 (2011).
 - [14] Y. Liu, G. Bartal, D. A. Genov, and X. Zhang, *Phys. Rev. Lett.* **99**, 153901 (2007).
 - [15] F. Ye, D. Mihalache, B. Hu, and N. C. Panou, *Phys. Rev. Lett.* **104**, 106802 (2010); *Opt. Lett.* **36**, 1179 (2011).

- [16] C. Jiang, S. Markutsya, Y. Pikus, and V. V. Tsukruk, *Nature Mater.* **3**, 721 (2004).
- [17] Z. Jakšić, S. M. Vuković, J. buha, and J. Matovic, *J. Nanophotonics* **5**, 051818 (2011).
- [18] Y. Fedutik, V. Temnov, U. Woggon, E. Ustinovich, and M. Artemyev, *J. Am. Chem. Soc.* **129**, 14939 (2007).
- [19] J. Rho, Z. Ye, Y. Xiong, X. Yin, Z. Liu, H. Choi, G. Bartal, X. Zhang, *Nature Comm.* **1**, 143 (2010).
- [20] P. B. Johnson and R. W. Christy, *Phys. Rev. B* **6**, 4370 (1972).
- [21] E. J. Smith, Z. Liu, Y. Mei, and O. G. Schmidt, *Nano Lett.* **10**, 1 (2010).
- [22] S. L. Chuang, *J. Lightwave Technol.* **5**, 5 (1987); **5**, 174 (1987).